Tempo and Pattern of Avian Brain Size Evolution

Highlights

- Dinosaurs and early birds had similar relative brain sizes

- Major shifts in brain-body integration occur in the aftermath of the K-Pg extinction

- Rates of brain-body evolution are highest in non-avian dinosaurs, early-diverging birds, parrots, and crows

- Corvids, like hominins, evolved larger relative brains and bodies simultaneously

Authors

Daniel T. Ksepka, Amy M. Balanoff,
N. Adam Smith, ..., Lindsay E. Zanno,
Erich D. Jarvis, Jeroen B. Smaers

Correspondence

dksepka@brucemuseum.org

In Brief

Ksepka et al. reconstruct brain-body scaling in a study of >2,000 birds and non-avian dinosaurs. Their results show that avian brain size evolution was profoundly impacted by the K-Pg mass extinction, in the aftermath of which many clades achieved larger relative brain sizes via body size reduction.

CellPress

Article

Tempo and Pattern of Avian Brain Size Evolution

Daniel T. Ksepka,[1,2,3,4,42,43,]* Amy M. Balanoff,[5,6,42] N. Adam Smith,[3,7,42] Gabriel S. Bever,[6,8] Bhart-Anjan S. Bhullar,[9] Estelle Bourdon,[10] Edward L. Braun,[11] J. Gordon Burleigh,[11] Julia A. Clarke,[12] Matthew W. Colbert,[12] Jeremy R. Corfield,[13] Federico J. Degrange,[14] Vanesa L. De Pietri,[15] Catherine M. Early,[16,17] Daniel J. Field,[18] Paul M. Gignac,[19] Maria Eugenia Leone Gold,[6,20] Rebecca T. Kimball,[21] Soichiro Kawabe,[22] Louis Lefebvre,[23] Jesús Marugán-Lobón,[24,25] Carrie S. Mongle,[26] Ashley Morhardt,[27] Mark A. Norell,[6] Ryan C. Ridgely,[28] Ryan S. Rothman,[29] R. Paul Scofield,[15] Claudia P. Tambussi,[14] Christopher R. Torres,[30] Marcel van Tuinen,[31] Stig A. Walsh,[32] Akinobu Watanabe,[6,33,34] Lawrence M. Witmer,[28] Alexandra K. Wright,[35] Lindsay E. Zanno,[36,37] Erich D. Jarvis,[38,39] and Jeroen B. Smaers[40,41,42]

[1]Bruce Museum, Greenwich, CT 06830, USA
[2]Department of Ornithology, American Museum of Natural History, New York, NY 10024, USA
[3]Division of Science and Education, Field Museum of Natural History, Chicago, IL 60605, USA
[4]Department of Paleobiology, Smithsonian Institution, Washington, DC 20013, USA
[5]Department of Psychological and Brain Sciences, Johns Hopkins University, Baltimore, MD 21218, USA
[6]Division of Paleontology, American Museum of Natural History, New York, NY 10024, USA
[7]Campbell Geology Museum, Clemson University, Clemson, SC 29634, USA
[8]Center for Functional Anatomy and Evolution, Johns Hopkins University School of Medicine, Baltimore, MD 21205, USA
[9]Department of Geology & Geophysics and Peabody Museum of Natural History, Yale University, New Haven, CT 06511, USA
[10]UMR 7205 Laboratoire Informatique et Systématique, Muséum National d'Histoire Naturelle, 75005 Paris, France
[11]Department of Biology, University of Florida, Gainesville, FL 32611, USA
[12]The Jackson School of Geosciences, The University of Texas at Austin, Austin, TX 78712, USA
[13]Salisbury University, Salisbury, MD 28101, USA
[14]Centro de Investigaciones en Ciencias de la Tierra, UNC, CONICET, Córdoba X5016GCA, Argentina
[15]Canterbury Museum, Christchurch 8013, New Zealand
[16]Department of Biological Sciences, Ohio University, Athens, OH 45701, USA
[17]Florida Museum of Natural History, University of Florida, Gainesville, FL 32611, USA
[18]Department of Earth Sciences, University of Cambridge, Cambridge CB2 3EQ, UK
[19]Oklahoma State University Center for Health Sciences, Tulsa, OK 74107, USA
[20]Biology Department, Suffolk University, Boston, MA 02108, USA
[21]Department of Anatomical Sciences, Stony Brook University, Stony Brook, NY 11794, USA
[22]Fukui Prefectural Dinosaur Museum, 51-11 Terao, Muroko, Katsuyama, Fukui 911-8601, Japan
[23]Department of Biology, McGill University, Montréal, QC H3A 0G4, Canada
[24]Departamento de Biología, Universidad Autónoma de Madrid, 28049 Madrid, Spain
[25]Dinosaur Institute, Natural History Museum of Los Angeles, Los Angeles, CA 90007, USA
[26]Division of Anthropology, American Museum of Natural History, New York, NY 10024, USA
[27]Washington University School of Medicine in St. Louis, St. Louis, MO 06130, USA
[28]Department of Biomedical Sciences, Ohio University Heritage College of Osteopathic Medicine, Ohio Center for Ecology and Evolutionary Studies, Athens, OH 45701, USA
[29]Interdepartmental Doctoral Program in Anthropological Sciences, Stony Brook University, Stony Brook, NY 11794, USA
[30]Department of Integrative Biology, University of Texas at Austin, Austin, TX 78712, USA
[31]Department of Otorhinolaryngology, University Medical Center, Groningen 9713, the Netherlands
[32]National Museum of Scotland, Edinburgh EH1 1JF, UK
[33]Department of Anatomy, New York Institute of Technology, College of Osteopathic Medicine, Old Westbury, NY 11568, USA
[34]Life Sciences Department, Vertebrates Division, Natural History Museum, London SW7 5BD, UK
[35]Sea Mammal Research Unit, University of St Andrews, St Andrews, KY16 9XL, UK
[36]Paleontology, North Carolina Museum of Natural Sciences, Raleigh, NC 27601, USA
[37]Department of Biological Sciences, North Carolina State University, Raleigh, NC 27695, USA
[38]The Rockefeller University, New York, NY 10065, USA
[39]The Howard Hughes Medical Institute, Chevy Chase, MD 20815, USA
[40]Department of Anthropology, Stony Brook University, Stony Brook, NY 11794, USA
[41]Division of Anthropology, American Museum of Natural History, New York, NY 10024, USA
[42]These authors contributed equally
[43]Lead Contact
*Correspondence: dksepka@brucemuseum.org
https://doi.org/10.1016/j.cub.2020.03.060

SUMMARY

Relative brain sizes in birds can rival those of primates, but large-scale patterns and drivers of avian brain evolution remain elusive. Here, we explore the evolution of the fundamental brain-body scaling relationship across the origin and evolution of birds. Using a comprehensive dataset sampling > 2,000 modern birds, fossil birds, and

theropod dinosaurs, we infer patterns of brain-body co-variation in deep time. Our study confirms that no significant increase in relative brain size accompanied the trend toward miniaturization or evolution of flight during the theropod-bird transition. Critically, however, theropods and basal birds show weaker integration between brain size and body size, allowing for rapid changes in the brain-body relationship that set the stage for dramatic shifts in early crown birds. We infer that major shifts occurred rapidly in the aftermath of the Cretaceous-Paleogene mass extinction within Neoaves, in which multiple clades achieved higher relative brain sizes because of a reduction in body size. Parrots and corvids achieved the largest brains observed in birds via markedly different patterns. Parrots primarily reduced their body size, whereas corvids increased body and brain size simultaneously (with rates of brain size evolution outpacing rates of body size evolution). Collectively, these patterns suggest that an early adaptive radiation in brain size laid the foundation for subsequent selection and stabilization.

INTRODUCTION

Significant deviations from "universal" anatomical scaling relationships provide fundamental insights into common growth laws and thus help identify major shifts in evolutionary patterns and their causative mechanisms [1–6]. Departures from standard scaling relationships generally align with changes in genetic and developmental regulation [7] and thereby might reveal changes in adaptive profile. Such allometric deviations shape the direction of trait variation on a macroevolutionary scale and consequently underlie much of modern phenotypic diversity [8].

Brain size is one of the most widely studied traits in this framework and has been correlated with major evolutionary innovations, such as enhanced sensory capabilities, cognition, social complexity, flight, and environmental adaptability [1–5, 9–15]. Brain size within vertebrates typically scales allometrically, and differences in relative brain size can stem from changes in body size, brain size, or both [1, 15]. Disentangling these variables is key to reconstructing the tempo and pattern of brain evolution. However, a synthetic understanding of brain-body size scaling is not attainable by studying extant taxa alone. Fossils are crucial, as non-avian dinosaurs provide a window into changes occurring during the phylogenetic interval of "miniaturization" preceding the evolution of flight [16, 17] and help anchor estimates of ancestral states given the paucity of endocasts available from Mesozoic birds. Moreover, extinct birds, especially flightless taxa (e.g., moa and dodo), might provide insights into encephalization patterns, given that the loss of flight is often accompanied by a rapid increase in body size [18].

Traits, such as brain size, can be mapped across phylogeny, but properly interpreting trait-mapping algorithms can be challenging, especially when the traits of interest share scaling relationships that might themselves be under selection. We implement a suite of methods that allows us to untangle the effects of changes in brain-body size relationships by considering that both the intercept (mean deviation from the common scaling relationship) and slope (co-variation of this relationship) can be under selection (e.g., [19, 20]). Shifts in intercept correspond to differences in mean relative brain size among taxa that share a given slope, whereas shifts in slope correspond to more (or less) rapid changes in brain volume relative to changes in body size [1]. Such changes can be quantified by identifying disparities in the intercept and slope of a phylogenetic regression between different groups. Furthermore, groups that exhibit a high accumulation of residual deviations provide more variation for

selection to act upon and can thereby be considered to be more evolutionarily flexible [20].

We assembled a brain endocast dataset sampling 284 extant bird species, 22 extinct bird species, and 12 non-avian theropod dinosaurs, which we combined with a sample of >1,900 extant species from the recent study of Sayol et al. [14] (Figure S1). The inclusion of fossil data has been shown to improve inferences of trait evolution [21, 22] and further allows us to answer questions about patterns of evolution in deep time. Our analyses utilize a two-phase approach. First, we use bivariate multi-regime Ornstein-Uhlenbeck (OU) methods [23–25] to identify where shifts in slope and intercept occur in the phylogeny. Second, we confirmed these shifts by using generalized least-squares phylogenetic analysis of co-variance (pANCOVA) [26, 27] and quantify strength of integration by using a Brownian motion rate comparison of allometric residuals among groups [28]. We further identify where in the phylogeny univariate shifts in body size and brain size have occurred by comparing phylogenetic means of brain and body size among allometric grades [26, 27] in order to estimate whether disproportionate changes in either brain size or body size have influenced allometric shifts in the brain-to-body size relationship.

RESULTS

Evolution of Brain-Body Allometry in Birds

Our OU and pANCOVA analyses identify large-scale allometric differences in the brain-body relationship across clades (Figure 1). The best-fit model identifies four slopes and eleven intercepts, which together comprise eleven grades (Figure 2; Tables 1 and S1). This multi-grade model shows a significantly better fit than a single-grade model ($F_{15,2} = 29.56$; $p < 0.001$) or to a model that includes only differences in intercepts ($F_{15,12} = 51.08$; $p < 0.001$). Mapping these scaling relationships across phylogeny, we identify evolutionary shifts away from the ancestral pattern of brain-body co-variation (slope shifts) along nine branches (Figure 1A, asterisks), with nine additional shifts to higher or lower intercepts without a change in slope.

Non-avian dinosaurs and basally diverging birds share a low ancestral slope. Yet, rates of relative brain size evolution are higher along the phylogenetic interval spanning non-avian theropods and the base of the crown bird radiation than for most of the later-diverging crown bird groups (Table 2). Among non-avian dinosaurs, there were three independent shifts in grade, all resulting in a higher intercept but no change in slope (Figures 1A and 3A) (shifts from purple grade to gray grade). One of these shifts
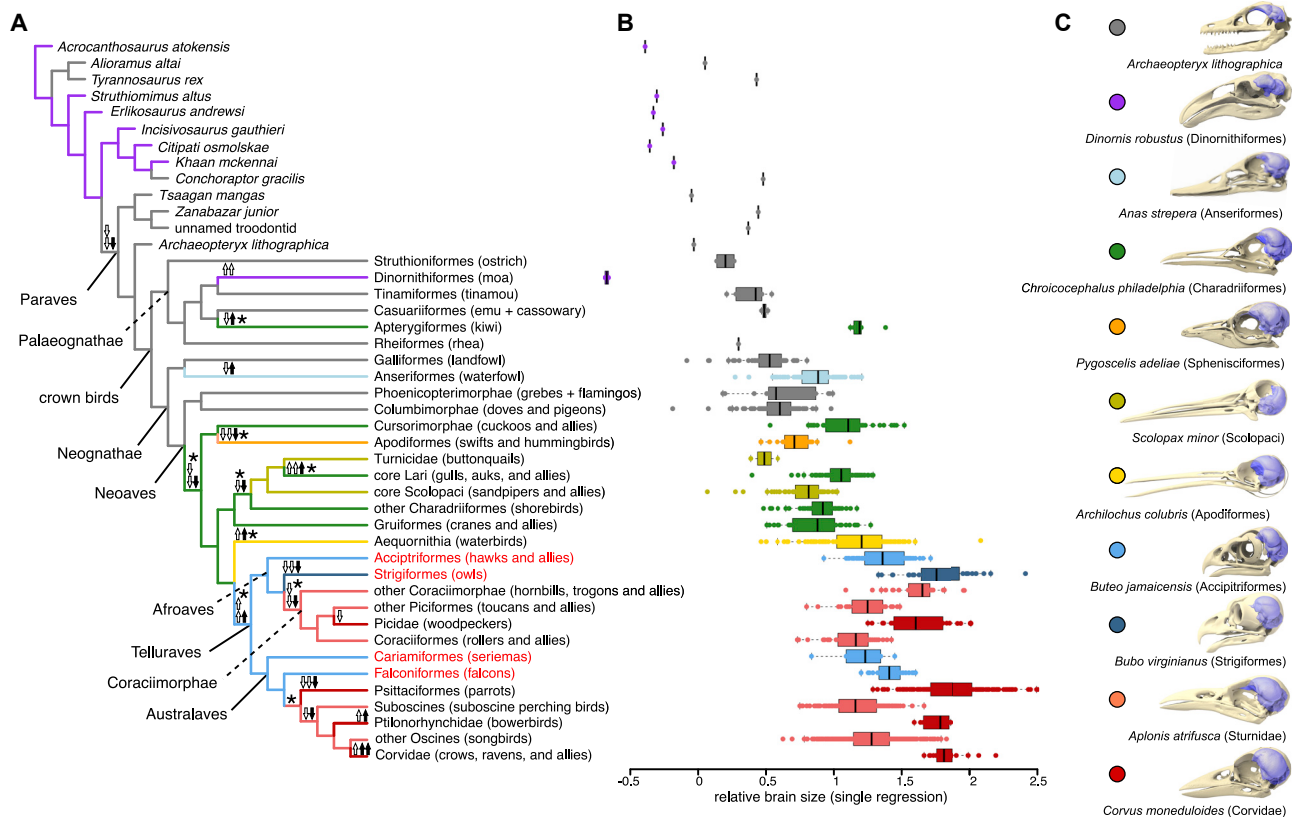
Figure 1. Avian Brain-Body Size Evolution

(A) Simplified phylogeny of non-avian theropods and birds using phylogenetic backbone from [29]. Branch colors correspond to the eleven significantly different adaptive grades ($F_{15,2} = 29.56$; p < 0.001; AICΔ = 343.53; AICω > 0.99) identified in this study. Changes in body size (white arrows) and brain volume (black arrows) resulting in grade shifts are indicated along the branches to which they pertain. Double arrows indicate one of these variables changing faster than the other after considering the allometric relationship between the two. Asterisks indicate shifts in slope. Predatory bird clades are indicated in red font.

(B) Brain size residuals standardized to a "one slope-one intercept" allometry to provide a simplified visualization of relative brain size.

(C) Skulls and endocasts of representative taxa from each of the eleven grades identified.

See Figure S1 for complete phylogeny and Figures S2 and S3 for results using alternate models.

occurs in Paraves (the clade uniting deinonychosaurian theropods and birds), giving rise to the grade that is retained in *Archaeopteryx* and deeply diverging crown birds, including Palaeognathae ("ratites" and tinamous), Galloanserae (landfowl and waterfowl), Phoenicopterimorphae (grebes and flamingos), and Columbimorphae (pigeons and allies). Three shifts in mean relative brain size occur within clades sharing the ancestral avian grade. Anseriformes (waterfowl) exhibit an increase in intercept but no significant change in slope (Figure 2A, teal regression). Apterygiformes (kiwi) show an increase in both intercept and slope, which results in these small, specialized ratites converging with the higher-slope grade characterizing many early-diverging clades of Neoaves (Figure 2B, green regression). Conversely, a decrease in intercept, indicating a pronounced decrease in mean relative brain size, is observed within Dinornithiformes (moa) (Figure 2A, purple regression).

The earliest shift to a higher slope occurs within Neoaves, along the branch uniting all neoavian birds except for the basally diverging Phoenicopterimorphae and Columbimorphae (Figures 1A and 3A). Within Neoaves, a pervasive trend of achieving even higher slopes via continued decrease in body size is

observed: this pattern occurs within Apodiformes (in hummingbirds and swifts), Charadriiformes (in sandpipers and buttonquails), and five times within Telluraves (see below). Aequornithia (waterbirds) contradict this general pattern and are unique in showing a pattern in which both body size and brain size increase in almost the same proportion. This nevertheless results in a higher slope because brain size is expected to increase at ~0.6 log-body size because of scaling relationships [1].

Interestingly, the branch leading to Telluraves ("higher landbirds") is characterized by a marked decrease in slope, which corresponds to a major increase in body size (Figures 1A and 3A). Both sides of the basal divergence in Telluraves are occupied by pairs of successively branching predatory clades [29] (Figure 1A, clades in red font), which share a low slope while maintaining a high intercept: Accipitriformes (hawks, vultures, and allies) and Strigiformes (owls) on the Afroaves side and Falconiformes (falcons) and Cariamiformes (seriemas and the extinct "terror birds") on the Australaves side. Owls notably retain the ancestral Telluraves slope but shift to a higher intercept. Subsequently, multiple nested shifts to higher grades occur within Afroaves and Australaves: Coraciimorphae (mousebirds, rollers, and allies) shift to a
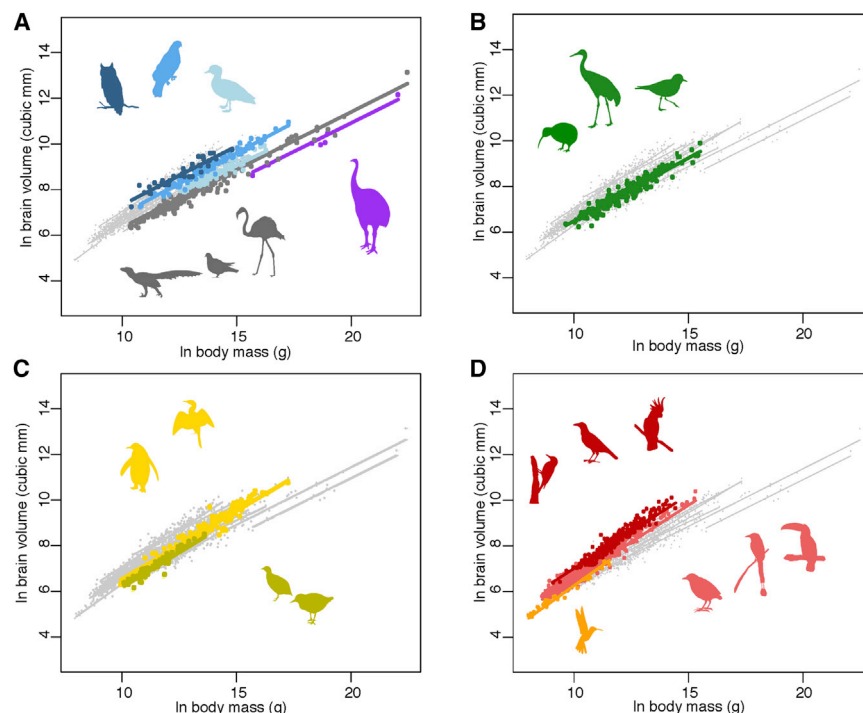
Figure 2. Adaptive Grades of Relative Brain Size

(A) Regressions for the five low-slope adaptive grades characterizing non-avian theropods, early-diverging birds (Palaeognathae, basal Neognathae), Anseriformes (waterfowl), and predatory telluravians.

(B) Regression for the intermediate-slope grade characterizing most neoavians and Apterygiformes (kiwi).

(C) Regressions for the two high-slope grades characterizing Aequornithia (waterbirds) and some Charadriiformes (shorebirds).

(D) Regressions for the three highest slope grades characterizing Apodiformes (swifts and hummingbirds), Coraciimorphae (mousebirds, rollers, and allies), Picidae (woodpeckers), Passeriformes (passerines), and Psittaciformes (parrots). Colors correspond to those used in Figure 1.

Silhouettes from http://phylopic.org; see Methods S1 for individual image credits.

higher slope and Picidae (woodpeckers) to a higher intercept in Afroaves, whereas Psittacopasserae (passerines and parrots) shift to a higher slope and Psittaciformes, Ptilonorhynchidae (bowerbirds), and Corvidae shift to a higher intercept in Australaves.

Two caveats should be recognized. First, the shift toward a higher intercept in bowerbirds coincides with a downward shift in slope, but because of low sample size (n = 10), there is not enough information to statistically establish whether bowerbirds align more with owls (Akaike information criterion [AIC] weight 0.526) or with parrots, corvids, and woodpeckers (AIC weight 0.473). Because bowerbirds are nested well within Passeriformes, we consider it more parsimonious to assume that they share the ancestral passerine slope and are thus aligned with parrots, corvids, and woodpeckers (as depicted in Figures 1 and 2) but recognize that future work is needed to test this scenario. Second, although a single-slope regression is extremely useful for a heuristic visual comparison of relative brain size across all taxa (Figure 1B), this can result in underestimation/overestimation for specific taxa. For example, the single slope regression is an underestimation of the high slope shared by Coraciimorphae, so relative brain size will be overestimated in large-bodied taxa in that clade (e.g., hornbills).

Our results are robust to sampling and modeling assumptions: we recover the same major patterns when constraining the tree to accommodate a shift along the avian stem lineage, comparing "early" versus "late" radiating clades, and excluding fossil taxa (Figures S2–S3; Table S2).

Shifts in Brain Size-Body Size Integration Occur during the Paleogene Crown Bird Radiation

Among vertebrates, birds and mammals are exceptional in showing reduced allometric constraints on the brain-body relationship [31]. The strength of brain-body integration can be approximated by examining the rate of evolution of residual allometric deviations: higher rates indicate increased decoupling of the brain-body relationship. In our analysis, concomitant with shifts in brain-body allometry immediately after the Cretaceous-Paleogene (K-Pg) mass extinction, we observe a significant shift in brain-body integration. Intriguingly, this shift is toward lower rather than higher rates of evolution and thus implies a stronger degree of integration. Rates of brain-body size evolution are high in theropods and early-diverging crown birds (Palaeognathae, Galloanserae, Phoenicopteriformes, and Columbimorphae) and shift to significantly lower rates early in the Paleogene radiation of Neoaves (Table 2). Although a decrease in body size is an important factor in this rate decrease, this finding is not an artifact of including large-bodied non-avian dinosaurs: a significantly higher rate of evolution is observed in early diverging crown birds (Palaeognathae and Galloanserae) versus Neoaves in supplementary analyses including only extant taxa (rate ratio of 1.56; p < 0.001).

In contrast to the lower rates that characterize most neoavians, a shift toward the highest rate of relative brain size evolution identified across all birds takes place in corvids (Table 2). A marked decrease in the strength of brain-body integration might thus have facilitated selection for increased brain size in these birds. Significant but less dramatic rate shifts are observed in parrots, owls, and waterfowl (Table 2).

DISCUSSION

Diverse Patterns of Brain-Body Size Changes Underpin Allometric Shifts

Our findings reveal complex patterns in the evolution of avian brain-body allometry. The initial shift to a higher grade in the expansive neoavian radiation appears to have been driven by body size decrease greatly outpacing brain volume decrease, resulting in larger average brain volumes at a given body mass (Table 3). Subsequently, at the base of the telluravian landbird radiation, the opposite pattern is observed, with a marked increase in

Table 1. Regression Parameters of All Grades Identified in the Primary Analysis

Grade	Slope	Slope SE	Intercept	Intercept SE
Non-avian theropods (purple)	0.499	0.017	0.92	0.344
Paraves, including early birds (gray)	0.504	0.010	1.309	0.216
Anseriformes: waterfowl (teal)	0.473	0.024	1.972	0.362
"Intermediate" Neoaves (green)	0.555	0.016	0.925	0.214
Apodiformes: swifts and hummingbirds (orange)	0.716	0.024	−0.862	0.250
Charadriiformes (part): sandpipers and buttonquail (gold)	0.613	0.001	0.002	0.091
Aequornithia: waterbirds (yellow)	0.595	0.019	0.544	0.275
Birds of prey: hawks, falcons, seriemas (light blue)	0.521	0.018	1.785	0.281
Strigiformes: owls (dark blue)	0.516	0.031	2.159	0.396
Coraciimorphae: rollers and allies (pink)	0.640	0.015	0.145	0.175
Picidae: woodpeckers (red, part)	0.700	0.045	−0.097	0.488
Psittaciformes: parrots (red, part)	0.635	0.017	0.795	0.236
Passeriformes: passerines (pink, part)	0.647	0.007	0.201	0.111
Ptilonorhynchidae: bowerbirds (red, part)	0.547	0.067	1.743	1.035
Corvidae: crows and ravens (red, part)	0.660	0.018	0.435	0.241

Values derived from phylogenetic Generalized Least Squares (pGLS) analyses with lambda transformation. Colors refer to those depicted in Figure 2. The individual clades that contribute to the highest slope grades are broken out separately for illustrative purposes.

body size outpacing a simultaneous increase in brain size. This coincides with a shift to a carnivorous diet that characterizes four basally diverging telluravian clades (Accipitriformes, Strigiformes, Falconiformes, and Cariamiformes). Despite having relatively large brains in comparison to other neoavians, all four predatory clades share the low slope ancestral for birds, indicating a lower rate of brain evolution relative to body size evolution. This pattern is particularly striking as it parallels well-characterized patterns in mammalian carnivorans, in which changes in relative brain size have been attributed largely to body size evolution rather than selection for neuronal capacity [15]. Our data suggest that strong body size selection in raptorial birds linked to their preferred prey classes (e.g., small rodents versus large waterfowl) might have been the most important driver of the brain-body relationship in early Telluraves.

Intriguingly, parallel shifts toward higher slopes accompany the independent transitions away from predatory ecologies in the two major clades of Telluraves. In Afroaves, the

Coraciimorphae show a secondary decrease in body size that leads them to exhibit a higher slope, and in Australaves, this pattern is mirrored by a secondary decrease in body size accompanying a shift to a higher slope in Psittacopasserae. Further decreases in body size leading to higher intercept grades occur within Picidae (in Afroaves) and Psittaciformes (in Australaves). Afroaves and Australaves are not complete parallels, however, as parrots achieve much larger relative brain sizes than woodpeckers, and the second-largest-brained bird clade (Corvidae) also evolves within Australaves via a unique pathway. Corvids achieve a higher intercept grade by simultaneous increase in body size and brain size, with the latter greatly outstripping the former. Parrots and corvids are unique not only for their large brains but also for exhibiting the highest inferred rates of brain-body evolution within Neoaves (Table 2).

Not all shifts, however, led to larger relative brain sizes. In some species of moa, relative brain size dropped to a level comparable with that of non-avian theropods because body size increased dramatically with less concomitant change in brain volume (Table 3). Such dichotomies in the patterns of brain and/or body size underpinning allometric shifts highlight that changes in encephalization are not unequivocally related to selection on brain size alone [15, 31].

Inferring Patterns and Drivers of Avian Brain Evolution

We infer that a general trend toward larger relative brain sizes along the backbone of the crown bird tree (Figures 1B and 3B) was initially driven primarily by selection for smaller body size. However, selection for brain size appears to take over as the primary driver in the largest-brained birds. Counterintuitively, rates of evolution are higher along the phylogenetic interval spanning non-avian theropods and the base of the crown bird radiation and slow down within Neoaves (Table 2). This observation might be in part because of body size not being constrained by the aerodynamic demands of flight in non-avian dinosaurs. However, this pattern remains when fossil taxa are excluded. An early interval during which a high rate of evolution prevailed might have set the stage for selection to act on a wider range of encephalization levels in early crown birds. Rates of evolution appear to have stabilized over time, whereas directional selection acted on individual clades. This interval was punctuated by the more recent, pronounced rate increases in corvids, parrots, and owls.

Our inference of a shared scaling relationship between theropods, *Archaeopteryx*, and basally diverging crown birds (i.e., most palaeognaths, landfowl, and basal neoavians) is in concordance with previous studies, which found that, despite a trend toward body size reduction and the acquisition of flight having occurred along the avian stem lineage, there is no evidence for major shifts in relative brain size associated with the divergence of *Archaeopteryx* (i.e., near the origin of powered flight) or the origin of crown birds [32, 33]. Although this does not preclude morphological changes in regional brain shape (which is often plastic even within modern bird families), previous studies have concluded that no significant changes in the relative volume of the cerebrum or cerebellum occurred along the transition from Paraves to basal crown birds [33].

It is compelling to note that only three grade shifts are inferred across the phylogenetic interval spanning Paraves to

Table 2. Comparison of Rate of Brain-Body Evolution between Groups

σ^2		Thero.	Psitt.	Strig.	Char1.	Anser.	Para.	BoP	Pic.	Aequ.	Ptil.	Neo.	Cora.	Pass.	Apod.	Char2.
0.0157	Corvidae	3.17	3.87[a]	4.59[a]	4.63[a]	5.17[a]	7.32[a]	7.66[a]	8.06[a]	9.45[a]	11.03[a]	11.21[a]	12.76[a]	13.03[a]	17.73[a]	18.64[a]
0.0049	non-avian theropods (purple)	x	1.22	1.45	1.46	1.63	2.31	2.41	2.54	2.98	3.48	3.54	4.03[a]	4.11[a]	5.59[a]	5.88[a]
0.0041	Psittaciformes	x	x	1.18	1.19	1.33	1.89[a]	1.98[a]	2.08[a]	2.44[a]	2.85[a]	2.89[a]	3.29[a]	3.36[a]	4.58[a]	4.81[a]
0.0034	Strigiformes	x	x	x	1.01	1.13	1.60	1.67	1.76	2.06[a]	2.41	2.44[a]	2.78[a]	2.84[a]	3.87[a]	4.07[a]
0.0034	Charadriiformes (most species)	x	x	x	x	1.12	1.58[a]	1.66[a]	1.74	2.04[a]	2.38	2.42[a]	2.76[a]	2.82[a]	3.83[a]	4.03[a]
0.0030	Anseriformes	x	x	x	x	N/A	1.42[a]	1.48	1.56	1.83[a]	2.13	2.17[a]	2.47[a]	2.52[a]	3.43[a]	3.61[a]
0.0021	Paraves/early birds (gray)	x	x	x	x	x	x	1.05	1.10	1.29	1.51	1.53[a]	1.74[a]	1.78[a]	2.42[a]	2.55[a]
0.0021	birds of prey	x	x	x	x	x	x	x	1.05	1.23	1.44	1.46[a]	1.67[a]	1.70[a]	2.32[a]	2.44[a]
0.0019	Picidae	x	x	x	x	x	x	x	x	1.17	1.37	1.39	1.58	1.62	2.20[a]	2.31[a]
0.0017	Aequornithia	x	x	x	x	x	x	x	x	x	1.17	1.19	1.35	1.38[a]	1.88[a]	1.97[a]
0.0014	Ptilonorhynchidae	x	x	x	x	x	x	x	x	x	x	1.02	1.16	1.18	1.61	1.69
0.0014	"intermediate" Neoaves (green)	x	x	x	x	x	x	x	x	x	x	x	1.14	1.16	1.58	1.66[a]
0.0012	Coraciimorphae	x	x	x	x	x	x	x	x	x	x	x	x	1.02	1.39	1.46
0.0012	Passeriformes	x	x	x	x	x	x	x	x	x	x	x	x	x	1.36	1.43
0.0009	Apodiformes	x	x	x	x	x	x	x	x	x	x	x	x	x	x	1.05
0.0008	Charadriiformes (sandpipers/ buttonquail)	x	x	x	x	x	x	x	x	x	x	x	x	x	x	x

Values represent ratios between group in first column and other groups. Abbreviations are as follows: Thero, non-avian theropods; Psitt, Psittaciformes; Strig, Strigiforms; Char1, Charadriiformes (most species); Anser, Anseriformes; Para, Paraves/early birds; BoP, birds of prey; Pic, Picidae; Aequ, Aequornithia; Ptil, Ptilonorhynchidae; Neo, "intermediate" Neoaves; Cora, Coraciimorphae; Pass, Passeriformes; Apod, Apodiformes; Char2, Charadriiformes (sandpipers/buttonquail). An "x" indicates "not applicable."
[a]Statistically significant ($p < 0.05$) differences between groups.

Neoaves, and only one of these (that in Anseriformes) is inferred to have taken place in the Cretaceous. In contrast, nine grade shifts, including seven resulting in new slopes, are inferred to have taken place during the Paleocene (Figure 3A). Thus, we infer that the most profound shifts in both brain-body size co-variation and relative brain size occurred not at the origin of flight or the appearance of crown birds but rather during the major ecological radiation of Neoaves after the K-Pg mass extinction [34–36]. This pattern aligns with the principles of adaptive radiation, in which early diversification is followed by directional changes in adaptive profile and slowdowns in rates of evolution [37].

Indeed, the K-Pg mass extinction might have set the stage for the diversification of Neoaves by providing a sustained period of environmental disruption. A classic explanation for the evolution of large brains is the cognitive buffer hypothesis [9, 10], which posits that large brains provide a buffer against frequent or unexpected environmental changes via enhanced capacity for flexible behavioral responses. Island-dwelling bird species consistently evolve larger relative brain sizes compared with that of their mainland relatives, a trend that has been interpreted as an adaptation to being restricted to environments in which conditions might often fluctuate dramatically [14]. This kind of environmental scenario occurred on a grand scale in the aftermath of the K-Pg mass extinction. On a more general level, large relative brain size is correlated with higher diversification rates in birds in

such a way as to be additive with other intrinsic or extrinsic factors affecting diversification [13]. Our results suggest that the aftermath of the K-Pg mass extinction created conditions ripe for the preferential survival and subsequent diversification of larger-brained birds. The impact on present day species richness and brain size diversity is evident in the larger range of overall relative brain sizes exhibited by Neoaves (>10,000 extant species) versus the more restricted range in basally diverging Palaeognathae and Galloanserae (~500 extant species; Figure 4).

Our results demonstrate that, despite diverging from non-avian dinosaurs ~150 mya, birds only reached their apex in relative brain size recently, when crown corvids and crown parrots radiated during the Neogene [38] (Figure 4). The finding that these taxa share both the highest inferred rates of brain-body evolution among Neoaves and the steepest allometric slopes among all birds raises the question of what common factors might underlie their shared trajectories. Parrots, oscine song-birds (including corvids), and hummingbirds (Trochilidae) are the only major groups of birds known to be capable of vocal learning, an ability controlled by additional brain pathways not found in other birds [39]. This complex behavior could represent a plausible driver of increased brain size in parrots. However, the case is more complicated within oscine songbirds and hummingbirds. Most oscines share the same ancestral slope as sub-oscines, almost all of which lack vocal learning. Hummingbirds likewise share the same ancestral slope as the non-vocal
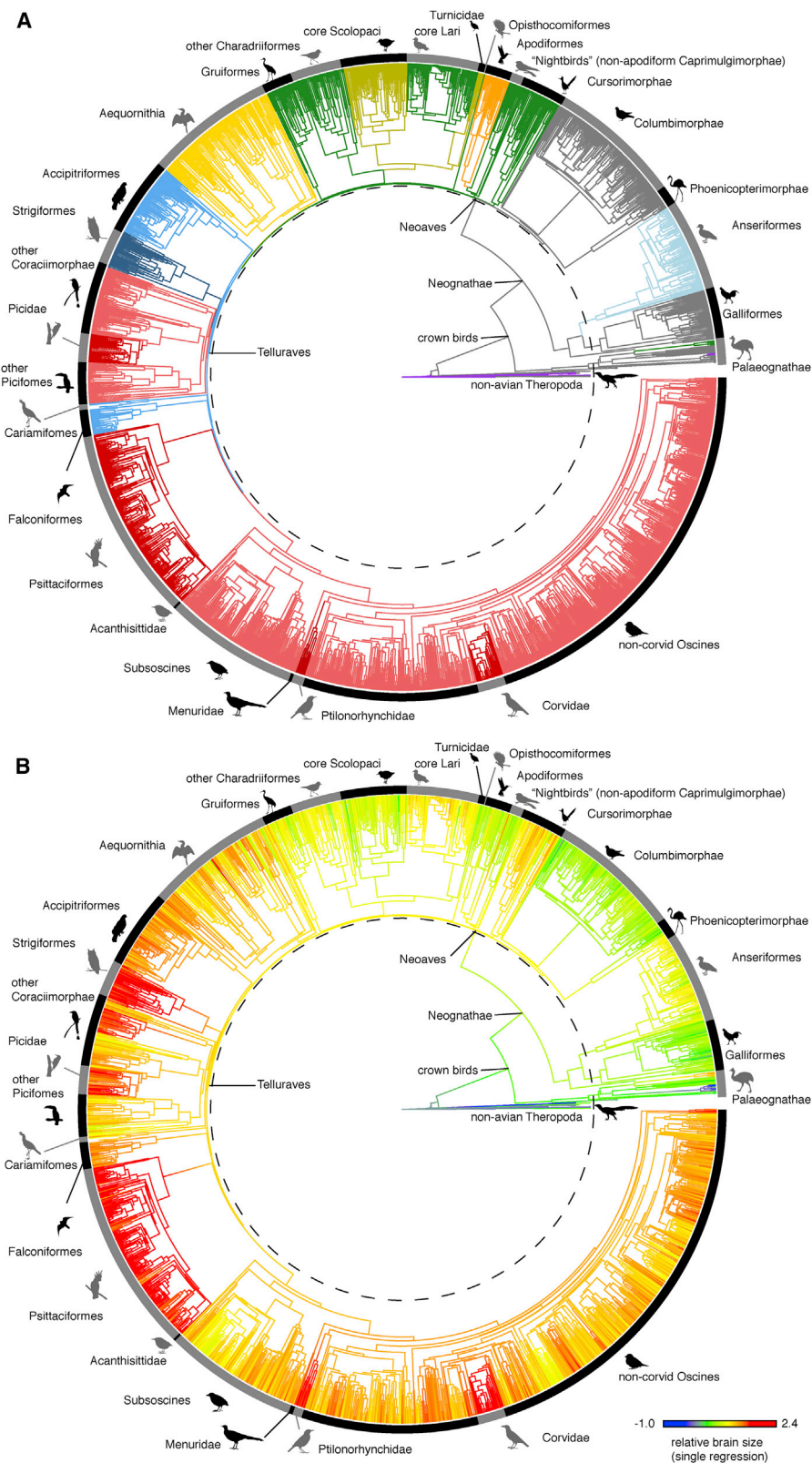
Figure 3. Patterns and Rates of Relative Brain Size Evolution

(A) Time-calibrated phylogeny of theropods and birds included in the endocast dataset illustrating the eleven brain-body size grades identified in this study.

(B) Ancestral state estimation [30] of brain size residuals standardized to a "one slope-one intercept" allometry.

Colors in (A) correspond to the adaptive grades illustrated in Figure 1. Dashed line in (A) and (B) indicates the K-Pg boundary.
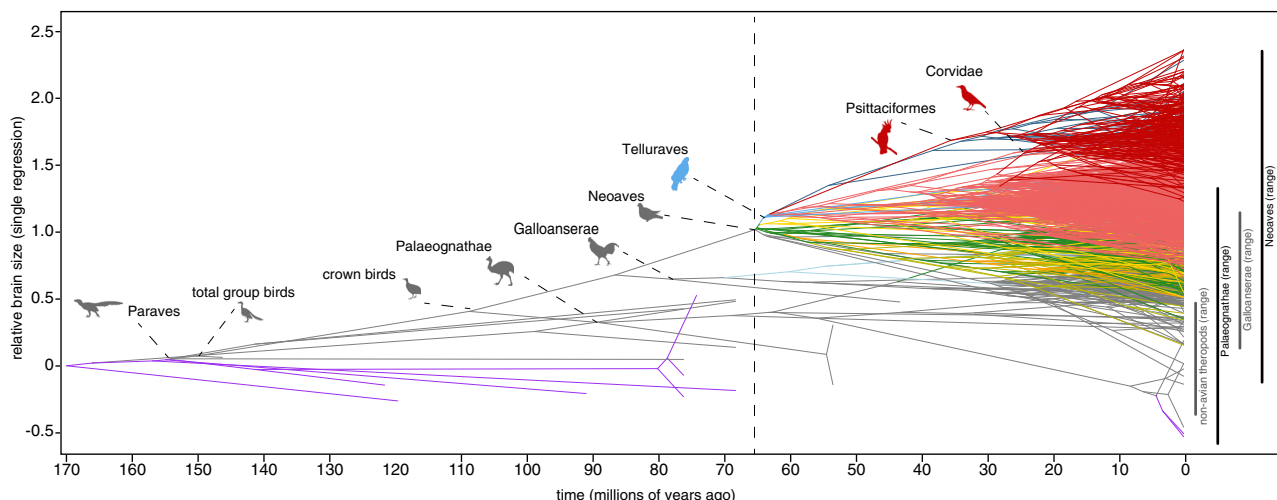
Figure 4. Evolution of Variation in Relative Brain Size
Phenogram showing relative brain size over time in non-avian theropods and birds. Colors correspond to the adaptive grades illustrated in Figure 1. Dashed line indicates the K-Pg boundary. Silhouettes are from phylopic.org, see Supplementary Information for individual image credits.

learning swifts. Although hummingbirds have exceptionally large brains as a raw proportion of body size, this appears to be almost exclusively an effect of negative allometry (i.e., smaller birds are expected to have proportionally larger brains). Thus, hummingbirds fall comfortably within the range of relative brain sizes observed in other early-diverging clades of Neoaves.

Recent studies suggest that high levels of encephalization might be due to differential growth of individual brain regions as opposed to their concerted evolution as well as some degree of modular evolution of associative pallial area [33, 40–42]. This hypothesis is supported by the observation that proportions of major neuroanatomical divisions vary widely in size among different groups of large-brained birds [40, 43–45]. Owls show an expanded visual Wulst [46]. Although this structure is part of the cerebrum, it serves a primarily sensory rather than associative function. Waterbirds exhibit an increase in the relative size of the cerebellum [33]. Parrots and oscine songbirds are similar to mammals in that their high encephalization values are primarily the product of increasing the relative size of the cerebral cortical regions [41]. Corvids provide an intriguing example of convergent brain evolution between birds and hominins, as these groups share a pattern in which brain volume and body size expanded simultaneously, with the former outpacing the latter [15].

Corvids and parrots exhibit impressive relative brain sizes, but basic volumetric indices likely underestimate their true neurological complexity. Parrots have recently been shown to have an additional vocal learning pathway not found in songbirds [47] and a disproportionately expanded telencephalic-midbrain-cerebellar circuit [47, 48]. Corvids and parrots together exhibit the highest known cerebral neuronal densities in birds, and raw neuronal counts in individual parrots and crows can actually rival those of some primates despite a smaller absolute brain size [49]. This increased neuron density has been suggested to accommodate enhanced brain pathways, such as those for vocal learning [49]. Thus, the increase

in cognitive complexity in parrots and corvids versus other birds might be a result of concomitant increases in not only relative brain volume but also neuron density, facilitating additional brain pathways or the elaboration or increased acuity of existing pathways.

Our data reveal the complex and dynamic evolutionary history of avian encephalization. This history includes high early rates of evolution that stabilized across the theropod-bird transition, a subsequent series of profound grade shifts as crown birds adapted to myriad ecologies early in the Cenozoic, and a culmination in which two groups—parrots and corvids—independently acquired relative brain sizes, neuronal densities, and sophisticated cognitive potential near the pinnacle of the vertebrate world.

STAR★METHODS

Detailed methods are provided in the online version of this paper and include the following:

- KEY RESOURCES TABLE
- LEAD CONTACT AND MATERIALS AVAILIBILITY
- METHOD DETAILS
  ○ Brain-volume and Body-mass Data
  ○ Phylogeny and Divergence Dating
- QUANTIFICATION AND STATISTICAL ANALYSIS
  ○ Characterizing Patterns of Allometric Integration
  ○ Assessing the Strength of Allometric Integration
  ○ Assessing Differential Changes in Brain and/or Body Size
- DATA AND CODE AVAILABILITY

SUPPLEMENTAL INFORMATION

Supplemental Information can be found online at https://doi.org/10.1016/j.cub.2020.03.060.

Table 3. Comparisons of Phylogenetic Means across Grades Identified in This Study versus Their Ancestral Grade

Grade	Brain Size			Body Size		
	Grade Average	Ancestral Grade	Ratio	Grade Average	Ancestral Grade	Ratio
Non-avian theropods and early-diverging birds (grey)	8.6	10.5	0.15	15.1	19.1	0.02
Dinornithiformes: moa	10.0	8.6	4.06	18.8	15.1	40.45
Apterygiformes: kiwi	9.2	8.6	1.82	14.5	15.1	0.55
Anseriformes: waterfowl	8.8	8.6	1.22	14.4	15.1	0.50
"Intermediate" Neoaves	7.9	8.6	0.50	12.5	15.1	0.07
Apodiformes: swifts and hummingbirds	6.1	7.9	0.17	9.8	12.5	0.07
Charadriiformes (part): sandpipers and buttonquail	7.0	7.9	0.41	11.4	12.5	0.33
Charadriiformes (part): other shorebirds	8.0	7.0	2.72	12.8	11.4	4.06
Aequornithia: waterbirds	8.8	7.9	2.46	13.6	12.5	3.00
Birds of prey: hawks, falcons, seriemas	9.3	7.9	4.06	14.4	12.5	6.69
Strigiformes: owls	8.6	9.3	0.50	12.5	14.4	0.15
Coraciimorphae: rollers and allies	7.3	9.3	0.14	11.2	14.4	0.04
Picidae: woodpeckers	7.4	7.3	1.11	10.6	11.2	0.55
Psittaciformes: parrots	8.8	9.3	0.61	12.6	14.4	0.17
Passeriformes: passerines	6.9	9.3	0.09	10.4	14.4	0.02
Ptilonorhynchidae: bowerbirds	8.2	6.9	3.67	11.9	10.3	4.95
Corvidae: crows and ravens	8.4	6.9	4.48	12.0	10.3	5.47

"Grade average" indicates the phylogenetic mean of brain and body size, and "ancestral grade" indicates the phylogenetic mean for the grade in which the target grade is nested. "Ratio" indicates the ratio of the (unlogged) phylogenetic mean value of the listed grade relative to that of its ancestral grade.

AUTHOR CONTRIBUTIONS

D.T.K., A.M.B., and N.A.S. organized the NESCent project that initiated this research. All authors except E.B., E.L.B., J.G.B., V.L.D.P., R.T.K., C.S.M., R.S.R., and S.K. participated in the planning of the project at the NESCent Catalysis Meeting. D.T.K., A.M.B., N.A.S., G.S.B., J.A.C., F.J.D., V.L.D.P., C.M.E., M.E.L.G., S.K., J.M.-L., A.M., M.A.N., R.C.R., R.P.S., C.P.T., M.v.T., L.M.W., S.A.W., A.K.W., and L.E.Z. contributed endocast data. J.G.B., E.L.B., R.T.K., and D.T.K. generated the dated phylogenies. J.B.S. completed the comparative analyses with R.S.R. and C.S.M. providing assistance. D.T.K., A.M.B., N.A.S., J.B.S., and E.D.J. drafted the manuscript, and all authors contributed to editing the paper.

DECLARATION OF INTERESTS

The authors declare no competing interests.

REFERENCES

1. Jerison, H. (1973). Evolution of the Brain and Intelligence (Academic).

2. Madden, J. (2001). Sex, bowers and brains. Proc. Biol. Sci. 268, 833–838.

3. Lefebvre, L., Nicolakakis, N., and Boire, D. (2002). Tools and brains in birds. Behaviour 139, 939–973.

4. Cnotka, J., Güntürkün, O., Rehkämper, G., Gray, R.D., and Hunt, G.R. (2008). Extraordinary large brains in tool-using New Caledonian crows (Corvus moneduloides). Neurosci. Lett. 433, 241–245.

5. Overington, S.E., Morand-Ferron, J., Boogert, N.J., and Lefebvre, L. (2009). Technical innovations drive the relationship between innovativeness and residual brain size in birds. Anim. Behav. 78, 1001–1010.

6. Thompson, D.W. (1917). On Growth and Form (Cambridge University).

7. Pélabon, C., Firmat, C., Bolstad, G.H., Voje, K.L., Houle, D., Cassara, J., Rouzic, A.L., and Hansen, T.F. (2014). Evolution of morphological allometry. Ann. N Y Acad. Sci. 1320, 58–75.

8. Voje, K.L., Hansen, T.F., Egset, C.K., Bolstad, G.H., and Pélabon, C. (2014). Allometric constraints and the evolution of allometry. Evolution 68, 866–885.

9. Allman, J.M., McLaughlin, T., and Hakeem, A. (1993). Brain structures and life-span in primate species. Proc. Natl. Acad. Sci. USA 90, 3559–3563.

10. Allman, J.M., and Martin, B. (1999). Evolving Brains (Scientific American Library).

11. Schuck-Paim, C., Alonso, W.J., and Ottoni, E.B. (2008). Cognition in an ever-changing world: climatic variability is associated with brain size in Neotropical parrots. Brain Behav. Evol. 71, 200–215.

12. Sayol, F., Maspons, J., Lapiedra, O., Iwaniuk, A.N., Székely, T., and Sol, D. (2016). Environmental variation and the evolution of large brains in birds. Nat. Commun. 7, 13971.

13. Sayol, F., Lapiedra, O., Ducatez, S., and Sol, D. (2019). Larger brains spur species diversification in birds. Evolution 73, 2085–2093.

14. Sayol, F., Downing, P.A., Iwaniuk, A.N., Maspons, J., and Sol, D. (2018). Predictable evolution towards larger brains in birds colonizing oceanic islands. Nat. Commun. 9, 2820.

15. Smaers, J.B., Dechmann, D.K., Goswami, A., Soligo, C., and Safi, K. (2012). Comparative analyses of evolutionary rates reveal different pathways to encephalization in bats, carnivorans, and primates. Proc. Natl. Acad. Sci. USA *109*, 18006–18011.

16. Turner, A.H., Pol, D., Clarke, J.A., Erickson, G.M., and Norell, M.A. (2007). A basal dromaeosaurid and size evolution preceding avian flight. Science *317*, 1378–1381.

17. Lee, M.S.Y., Cau, A., Naish, D., and Dyke, G.J. (2014). Dinosaur evolution. Sustained miniaturization and anatomical innovation in the dinosaurian ancestors of birds. Science *345*, 562–566.

18. McMahon, T.A., and Bonner, J.T. (1983). On Size and Life (Scientific American Library).

19. Stillwell, R.C., Shingleton, A.W., Dworkin, I., and Frankino, W.A. (2016). Tipping the scales: evolution of the allometric slope independent of average trait size. Evolution *70*, 433–444.

20. Smaers, J.B., Mongle, C.S., Safi, K., and Dechmann, D.K.N. (2019). Allometry, evolution and development of neocortex size in mammals. Prog. Brain Res. *250*, 83–107.

21. Slater, G.J., Harmon, L.J., and Alfaro, M.E. (2012). Integrating fossils with molecular phylogenies improves inference of trait evolution. Evolution *66*, 3931–3944.

22. Finarelli, J.A., and Flynn, J.J. (2006). Ancestral state reconstruction of body size in the Caniformia (Carnivora, Mammalia): the effects of incorporating data from the fossil record. Syst. Biol. *55*, 301–313.

23. Ingram, T., and Mahler, D.L. (2013). SURFACE: detecting convergent evolution from comparative data by fitting Ornstein-Uhlenbeck models with stepwise Akaike Information Criterion. Methods Ecol. Evol. *4*, 416–425.

24. Khabbazian, M., Kriebel, R., Rohe, K., and Ané, C. (2016). Fast and accurate detection of evolutionary shifts in Ornstein–Uhlenbeck models. Methods Ecol. Evol. *7*, 811–824.

25. Uyeda, J.C., and Harmon, L.J. (2014). A novel Bayesian method for inferring and interpreting the dynamics of adaptive landscapes from phylogenetic comparative data. Syst. Biol. *63*, 902–918.

26. Smaers, J.B., and Rohlf, F.J. (2016). Testing species' deviation from allometric predictions using the phylogenetic regression. Evolution *70*, 1145–1149.

27. Smaers, J.B., and Mongle, C.S. (2018). evomap: R package for the evolutionary mapping of continuous traits. https://github.com/JeroenSmaers/evomap.

28. Adams, D.C. (2014). Quantifying and comparing phylogenetic evolutionary rates for shape and other high-dimensional phenotypic data. Syst. Biol. *63*, 166–177.

29. Jarvis, E.D., Mirarab, S., Aberer, A.J., Li, B., Houde, P., Li, C., Ho, S.Y., Faircloth, B.C., Nabholz, B., Howard, J.T., et al. (2014). Whole-genome analyses resolve early branches in the tree of life of modern birds. Science *346*, 1320–1331.

30. Smaers, J.B., Mongle, C.S., and Kandler, A. (2016). A multiple variance Brownian motion framework for estimating variable rates and inferring ancestral states. Biol. J. Linn. Soc. Lond. *118*, 78–94.

31. Tsuboi, M., van der Bijl, W., Kopperud, B.T., Erritzøe, J., Voje, K.L., Kotrschal, A., Yopak, K.E., Collin, S.P., Iwaniuk, A.N., and Kolm, N. (2018). Breakdown of brain-body allometry and the encephalization of birds and mammals. Nat. Ecol. Evol. *2*, 1492–1500.

32. Balanoff, A.M., Bever, G.S., Rowe, T.B., and Norell, M.A. (2013). Evolutionary origins of the avian brain. Nature *501*, 93–96.

33. Balanoff, A.M., Smaers, J.B., and Turner, A.H. (2016). Brain modularity across the theropod-bird transition: testing the influence of flight on neuroanatomical variation. J. Anat. *229*, 204–214.

34. Feduccia, A. (1995). Explosive evolution in tertiary birds and mammals. Science *267*, 637–638.

35. Mayr, G. (2009). Paleogene Fossil Birds (Springer).

36. Field, D.J., Bercovici, A., Berv, J.S., Dunn, R., Fastovsky, D.E., Lyson, T.R., Vajda, V., and Gauthier, J.A. (2018). Early evolution of modern birds structured by global forest collapse at the end-Cretaceous mass extinction. Curr. Biol. *28*, 1825–1831.e2.

37. Gavrilets, S., and Losos, J.B. (2009). Adaptive radiation: contrasting theory with data. Science *323*, 732–737.

38. Prum, R.O., Berv, J.S., Dornburg, A., Field, D.J., Townsend, J.P., Lemmon, E.M., and Lemmon, A.R. (2015). A comprehensive phylogeny of birds (Aves) using targeted next-generation DNA sequencing. Nature *526*, 569–573.

39. Petkov, C.I., and Jarvis, E.D. (2012). Birds, primates, and spoken language origins: behavioral phenotypes and neurobiological substrates. Front. Evol. Neurosci. *4*, 12.

40. Iwaniuk, A.N., Dean, K.M., and Nelson, J.E. (2004). A mosaic pattern characterizes the evolution of the avian brain. Proc. Biol. Sci. *271* (*Suppl 4*), S148–S151.

41. Iwaniuk, A.N., Dean, K.M., and Nelson, J.E. (2005). Interspecific allometry of the brain and brain regions in parrots (psittaciformes): comparisons with other birds and primates. Brain Behav. Evol. *65*, 40–59.

42. Smaers, J.B., and Vanier, D.R. (2019). Brain size expansion in primates and humans is explained by a selective modular expansion of the cortico-cerebellar system. Cortex *118*, 292–305.

43. Kawabe, S., Shimokawa, T., Miki, H., Matsuda, S., and Endo, H. (2013). Variation in avian brain shape: relationship with size and orbital shape. J. Anat. *223*, 495–508.

44. Marugán-Lobón, J., Watanabe, A., and Kawabe, S. (2016). Studying avian encephalization with geometric morphometrics. J. Anat. *229*, 191–203.

45. Balanoff, A.M., and Bever, G.S. (2017). The role of endocasts in the study of brain evolution. In Evolution of Nervous Systems, *Volume 1*, J. Kaas, ed. (Elsevier), pp. 223–241.

46. Wylie, D.R., Gutiérrez-Ibáñez, C., and Iwaniuk, A.N. (2015). Integrating brain, behavior, and phylogeny to understand the evolution of sensory systems in birds. Front. Neurosci. *9*, 281.

47. Chakraborty, M., Walløe, S., Nedergaard, S., Fridel, E.E., Dabelsteen, T., Pakkenberg, B., Bertelsen, M.F., Dorrestein, G.M., Brauth, S.E., Durand, S.E., et al. (2015). Core and shell song systems unique to the parrot brain. PLoS ONE *10*, e0118496.

48. Chakraborty, M., and Jarvis, E.D. (2015). Brain evolution by brain pathway duplication. Philos. Trans. R. Soc. Lond. B Biol. Sci. *370*, 20150056.

49. Olkowicz, S., Kocourek, M., Lučan, R.K., Porteš, M., Fitch, W.T., Herculano-Houzel, S., and Němec, P. (2016). Birds have primate-like numbers of neurons in the forebrain. Proc. Natl. Acad. Sci. USA *113*, 7255–7260.

50. Iwaniuk, A.N., and Nelson, J.E. (2002). Can endocranial volume be used as an estimate of brain size in birds? Can. J. Zool. *80*, 16–23.

51. Balanoff, A.M., Bever, G.S., Colbert, M.W., Clarke, J.A., Field, D.J., Gignac, P.M., Ksepka, D.T., Ridgely, R.C., Smith, N.A., Torres, C.R., et al. (2016). Best practices for digitally constructing endocranial casts: examples from birds and their dinosaurian relatives. J. Anat. *229*, 173–190.

52. Dunning, J.B., Jr. (2008). CRC Handbook of Avian Body Masses, Second Edition (CRC).

53. Field, D.J., Lynner, C., Brown, C., and Darroch, S.A.F. (2013). Skeletal correlates for body mass estimation in modern and fossil flying birds. PLoS ONE *8*, e82000.

54. Christiansen, P., and Fariña, R.A. (2004). Mass prediction in theropod dinosaurs. Hist. Biol. *16*, 85–92.

55. Burleigh, J.G., Kimball, R.T., and Braun, E.L. (2015). Building the avian tree of life using a large-scale, sparse supermatrix. Mol. Phylogenet. Evol. *84*, 53–63.

56. Stamatakis, A. (2014). RAxML version 8: a tool for phylogenetic analysis and post-analysis of large phylogenies. Bioinformatics *30*, 1312–1313.

57. Sanderson, M.J. (2002). Estimating absolute rates of molecular evolution and divergence times: a penalized likelihood approach. Mol. Biol. Evol. *19*, 101–109.

58. Sanderson, M.J. (2003). r8s: inferring absolute rates of molecular evolution and divergence times in the absence of a molecular clock. Bioinformatics *19*, 301–302.

59. Turner, A.H., Makovicky, P.J., and Norell, M.A. (2012). A review of dromaeosaurid systematics and paravian phylogeny. Bull. Am. Mus. Nat. Hist. *371*, 1–206.

60. Maddison, W.P., and Maddison, D.R. (2015). Mesquite: a modular system for evolutionary analysis. Version 3.04. http://www.mesquiteproject.org.

61. Uyeda, J.F., Eastman, J., and Harmon, L. (2014). bayou: Bayesian fitting of Ornstein-Uhlenbeck models to phylogenies: R package version 1.0.1. http://CRAN.R-project.org/package=bayou.

62. Hansen, T.F. (1997). Stabilizing selection and the comparative analysis of adaptation. Evolution *51*, 1341–1351.

63. Uyeda, J.C., Pennell, M.W., Miller, E.T., Maia, R., and McClain, C.R. (2017). The evolution of energetic scaling across the vertebrate Tree of Life. Am. Nat. *190*, 185–199.

64. Ho, L.S.T., and Ané, C. (2014). Intrinsic inference difficulties for trait evolution with Ornstein-Uhlenbeck models. Methods Ecol. Evol. *5*, 1133–1146.

STAR★METHODS

KEY RESOURCES TABLE

REAGENT or RESOURCE	SOURCE	IDENTIFIER
Deposited Data		
Endocast volume and body mass dataset	This paper	Data S1
Constraint topology for analyses with Jarvis tree	This paper	Data S2
Taxon reconciliation table	This paper	Data S3
Unpruned, undated tree from ML analysis used as input for dating in r8s	This paper	Data S4
Final tree with brain and body mass data used in all downstream analyses	This paper	Data S5
Software and Algorithms		
R package 'bayou' V 2.1.1	https://github.com/uyedaj/bayou R package 'l1ou' V 1.40	N/A
R package 'l1ou' V 1.40	https://github.com/khabbazian/l1ou R package 'SURFACE' V 0.4-1	N/A
R package 'SURFACE' V 0.4-1	https://github.com/cran/surface R package 'evomap' V 2.0	N/A
R package 'evomap' V 2.0	https://github.com/JeroenSmaers/evomap	N/A
Mesquite V 3.03	http://mesquiteproject.org/	N/A
r8s	https://sourceforge.net/projects/r8s/	N/A

LEAD CONTACT AND MATERIALS AVAILIBILITY

Further information and requests for resources and reagents should be directed to and will be fulfilled by the Lead Contact, Daniel Ksepka (dksepka@brucemuseum.org). This study did not generate new unique reagents.

METHOD DETAILS

Brain-volume and Body-mass Data

We assembled a dataset of CT-rendered virtual endocasts to estimate brain volume, so as to facilitate sampling of rare and fossil taxa. Endocasts serve as a reliable proxy of the shape and volume of the brain in both birds and crownward non-avian theropods [50, 51]. We then combined this dataset with a recently published dataset based on lead-shot measurements of braincase volume [14]. Raw data and sources for taxa we sampled directly are provided in the electronic file Data S1. We obtained body mass data from a compendium [52] for most extant taxa. If the sex of a specimen was known, we used the average body mass of the appropriate sex when available. Otherwise, the species average was taken. For extinct birds where no body mass data were available from the literature, we applied body mass regressions from femur circumference [53]. For non-avian theropods, we applied a bivariate regression [54].

Phylogeny and Divergence Dating

As a phylogenetic backbone for the analysis of the endocast dataset (Data S2), we used a phylogeny based on whole genomes from nearly all 40+ avian orders [29]. In order to reconcile the taxa sampled in the constraint trees, the supermatrix, and our dataset, we substituted closely related species in a few cases. These are listed in Data S3. We generated a tree sampling ~6000 species using a pipeline approach [55] (Data S4). This tree was then dated using a penalized likelihood approach in r8s v.1.7 [56–58] with 21 fossil

calibrations (Methods S1). We then pruned extant taxa not represented in our dataset. Finally, extinct taxa for which no molecular data were available were grafted onto the tree based on a recent phylogeny for non-avian theropod taxa [59] or recent molecular/morphological phylogenies for each extinct bird species (see Data S1). Brain volume and body mass were then input for all taxa in MESQUITE 3.04 [60] (Data S5).

QUANTIFICATION AND STATISTICAL ANALYSIS

Characterizing Patterns of Allometric Integration

We estimated differences in slope and intercept of the brain-body relationship directly from the data using a Bayesian multi-regime Ornstein Uhlenbeck (OU) modeling approach [61]. The OU model assumes that the evolution of a continuous trait 'X' along a branch over time increment 't' is quantified as $dX(t) = \alpha[\theta - X(t)]dt + \sigma dB(t)$ [62]. Relative to the standard Brownian motion (BM) model ($dX(t) = \sigma dB(t)$), the OU model adds parameters that estimate mean trait value (θ) and the rate at which changes in mean values are observed (α). The inclusion of these additional parameters allows an appropriate differentiation between changes in the mean (θ and α) and variance (σ) of a trait over time and thus renders the OU model framework more appropriate than BM for modeling changes in the direction of trait evolution. Here we used a bivariate implementation of OU modeling that is explicitly geared toward estimating shifts in slope and intercept of evolutionary allometries by using reversible-jump Markov chain Monte Carlo machinery ('OUrjMCMC') [63]. We implemented this approach by combining 10 parallel chains of 2 million iterations each with a burn-in proportion of 0.3. We allowed only one shift per branch and the total number of shifts was constrained by means of a conditional Poisson prior with a mean equal to 2.5% of the total number of branches in the tree and a maximum number of shifts equal to 5%. Starting points for MCMC chains were set by randomly drawing a number of shifts from the prior distribution and assigning these shifts to branches randomly drawn from the phylogeny with a probability proportional to the size of the clade descended from that branch. The MCMC was initialized without any birth-death proposals for the first 10,000 generations to improve the fit of the model. The output of this procedure generates an estimate of a best-fit allometric model with posterior probabilities assigned to each shift in slope and/or intercept.

In part due to difficulties in parameter estimation intrinsic to OU modeling [64], the bivariate OUrjMCMC output may include false positives and/or false negatives. To identify false negatives, we ran a univariate OU model estimation procedure [23] on the residuals of each grade in order to detect shifts in mean. If such shifts in mean were detected, they were added as shifts in intercept to the allometric model (only the dinosaur grade with the lowest intercept in the sample was detected using this procedure). To identify false positives (including those that were added by the grade-specific univariate analyses), the allometric model was translated to a least-squares framework and used in a confirmatory analysis using phylogenetic ANCOVA ('pANCOVA') [26]. Even though pANCOVA uses a different evolutionary process than OU modeling (i.e., Brownian motion instead of Ornstein-Uhlenbeck), it is expected that grade membership as estimated by OU modeling is confirmed using least-squares analysis. Because Brownian motion assumes fewer statistical parameters, pANCOVA can be considered to be a conservative confirmatory test of the significance of grade membership as estimated by OU modeling.

Assessing the Strength of Allometric Integration

We compared rates of evolution among grades, applying a single intercept and single slope allometric model (one regression to fit entire sample), and between grades utilizing grade-specific allometric deviations. We compared rates after separating monophyletic clades for each grade (Table 2). We did not calculate rates for two clades (the moa *Emeus + Euryapteryx* and *Tyrannosaurus rex + Alioramus altai*) which include only two species as Brownian motion rates calculated based on so few data points cannot be considered valid. Finally, we compared rates between Neoaves (treating corvids as a separate group) and earlier radiating clades (Table S2).

Assessing Differential Changes in Brain and/or Body Size

To assess whether changes in the brain~body allometry were driven primarily by increase or decrease in either brain or body size, we calculated phylogenetic means for both brain size and body size for each of the allometric regimes identified by the best-fit allometric regime analysis described above using a procedure to calculate phylogenetic means [26], and implemented in the 'evomap' R package [27]. These analyses identify differences in mean brain and/or body size between groups of species. Results reveal the population averages in brain size and body size for the different allometric regimes. Comparing shifts in mean average brain size and body size across regimes provides an indication whether either shifts in brain size or body size primarily characterize shifts in allometric groups (Table 3). For example, in the analysis of the endocast dataset the allometric grade comprising corvids indicates a shift in (log) brain size of 1.5 and a shift in (log) body size of 1.7 relative to its ancestral grade (the ratio of unlogged size changes relative to their ancestral grade is 4.48 for brain size and 5.47 for body size, see Table 3). Considering that both the corvid grade and their ancestral grade indicate negative allometry (with slopes of 0.66 and 0.65; Table 1), the general expectation is that brain size changes at a slower pace relative to body size. Results for the shifts in brain and body size in corvids, however, indicate that brain size changes more than body size in this clade, even though there is also considerable change in body size. Given that changes in brain size and body size are both positive, these results prompt the interpretation that crows and ravens have increased both brain size and body size, but brain size more than body size given allometric expectations.

DATA AND CODE AVAILABILITY

Scripts for the R package Evomap are archived at GitHub (https://github.com) and can be downloaded in R using the code: require(devtools) install_github("JeroenSmaers/evomap")

Scripts for Bayou are archived at GitHub (https://github.com/uyedaj/bayou).

The input file for dating the tree in r8s is provided at Data S4 and the input data for the analyses of allometry are provided as Data S5.